MALT1 inhibition by MI-2 suppresses epithelial-to-mesenchymal transition and fibrosis by inactivating the NF-κB pathway in high glucose-treated HK-2 cells

YATING LAN[1], JIAN MA[2], HUIJUN CHEN[3], CHAOHONG LAN[4] and NA ZHAO[1-3]

[1]School of Clinical Medicine, Heilongjiang University of Chinese Medicine, Harbin, Heilongjiang 150040, P.R. China; [2]Department of Endocrinology, First Affiliated Hospital, Heilongjiang University of Chinese Medicine, Harbin, Heilongjiang 150040, P.R. China; [3]Department of Chinese Medicine Internal Medicine, Second Affiliated Hospital, Heilongjiang University of Chinese Medicine, Harbin, Heilongjiang 150008, P.R. China; [4]Internal Medicine Ward 5, Harbin Traditional Chinese Medicine Hospital, Harbin, Heilongjiang 150016, P.R. China

Received February 8, 2025; Accepted July 30, 2025

DOI: 10.3892/mmr.2025.13712

Abstract. Mucosa-associated lymphoid tissue lymphoma translocation protein 1 (MALT1) is a scaffold protein and protease that is associated with multiple biological processes, such as immune signaling transduction, inflammation and glucose variation. However, its implication in diabetic nephropathy (DN) is unclear. The present study aimed to investigate the dysregulation of MALT1 and the effect of its inhibition by MI-2 in high glucose-treated renal tubular epithelial cells. HK-2 cells were treated with 15 mM D-glucose [low-concentration glucose (LG) group] and 30 mM D-glucose [high-concentration glucose (HG)]. The negative control (NC) group consisted of cells cultured only with the standard medium. Subsequently, HK-2 cells under the HG condition were treated with 0, 1, 2 and 4 μM MI-2, an inhibitor of MALT1. Cell migration rate, invasive cell count, and the expression levels of vimentin, α-smooth muscle actin (α-SMA), fibronectin (FN) and collagen I were increased, whereas E-cadherin expression was decreased in the HG group compared with that in the NC group (all P<0.01), implying enhanced epithelial-to-mesenchymal transition (EMT) and fibrosis in the HG group. Furthermore, MALT1 was upregulated in the HG group compared with that in the NC group (P<0.01). Following MI-2 treatment in cells under the HG condition, the inhibitory effects of MI-2 on EMT, fibrosis and the NF-κB pathway were dose-dependent. Cell migration rate, invasive cell count and vimentin expression were reduced, whereas E-cadherin expression was elevated; furthermore, the expression levels of α-SMA, FN and collagen I were downregulated in the high concentration MI-2 (HC-MI-2) group compared with those in the HG group (all P<0.01). In addition, the NF-κB pathway was inactivated, as reflected by increased inhibitor of κB α expression and decreased phosphorylated-p65 expression in the HC-MI-2 group compared with in the HG group (both P<0.001). In conclusion, MALT1 inhibition by MI-2 suppresses EMT and fibrosis by inactivating the NF-κB pathway in HG-treated HK-2 cells, indicating its potency as a target for DN.

Introduction

Diabetic nephropathy (DN) is a prevalent and severe complication of diabetes mellitus, and it is the main cause of chronic kidney disease worldwide (1,2). Due to the complex and multifactorial pathogenesis of DN, the treatment of patients with DN is challenging (3,4). Notably, renal fibrosis is essential for the pathological process of DN (5,6), and epithelial-to-mesenchymal transition (EMT), which refers to the differentiation of epithelial cells into migratory and invasive mesenchymal cells, is considered a critical step in the development of renal fibrosis (7-10). Therefore, inhibiting EMT and renal fibrosis may contribute to suppressing the progression of DN.

Mucosa-associated lymphoid tissue lymphoma translocation protein 1 (MALT1) is a scaffold protein and protease regulating downstream signaling pathways (11-13). Previous studies have indicated that the inhibition of MALT1 has a suppressive effect on EMT and organ fibrosis (14,15). For example, a study suggested that MALT1 could facilitate EMT through regulation of EMT-transcription factors (14). Another study revealed that the inhibition of MALT1 reduces fibrosis, and this may be attributed to suppression of the NF-κB signaling pathway (15). Therefore, the inhibition of MALT1 could be considered a potential treatment target for DN. MI-2 is an irreversible small molecule inhibitor that combines with MALT1 and disrupts its protease function (16). However, to

Correspondence to: Dr Na Zhao, Department of Endocrinology, First Affiliated Hospital, Heilongjiang University of Chinese Medicine, 26 Heping Road, Harbin, Heilongjiang 150040, P.R. China
E-mail: zhaonadoc@163.com

Key words: mucosa-associated lymphoid tissue lymphoma translocation protein 1, high glucose-treated HK-2 cells, epithelial-to-mesenchymal transition, fibrosis, NF-κB pathway

the best of our knowledge, the role of MI-2 in attenuating the EMT of kidney cells or renal fibrosis to mitigate DN has not yet been demonstrated. Therefore, the current study aimed to investigate the effect of MALT1 inhibition by MI-2 on high glucose-induced EMT and fibrosis in HK-2 cells.

Materials and methods

Cell culture. HK-2 cells were purchased from Xiamen Yimo Biotechnology Co., Ltd. The cells were cultured in a special HK-2 culture medium (Wuhan Servicebio Technology Co., Ltd.) containing 5.6 mM D-glucose (MedChemExpress), pre-supplemented with 10% fetal bovine serum (FBS; Wuhan Pricella Biotechnology Co., Ltd.) and 1% penicillin/streptomycin solution (Wuhan Servicebio Technology Co., Ltd.).

Glucose treatment. HK-2 cells were cultured to 80% confluence in standard medium. Subsequently, the cells were treated with fresh medium plus either 15 mM D-glucose [low-concentration glucose (LG) group] or 30 mM D-glucose [high-concentration glucose (HG) group]. The negative control (NC) group consisted of cells cultured only with the standard medium. After being treated for 48 h at 37˚C, the cells were harvested for wound healing and invasion assays, immunofluorescence staining and western blotting.

MI-2 treatment. MI-2 (MedChemExpress), a MALT1 inhibitor, was used to suppress the protease function of MALT1. HK-2 cells were treated with medium containing 30 mM D-glucose and either 0, 1, 2 or 4 μM MI-2, and were named as the HG group, the low concentration MI-2 (LC-MI-2) group, the medium concentration MI-2 (MC-MI-2) group and the high concentration MI-2 (HC-MI-2) group, respectively. The wound healing and invasion assays, immunofluorescence staining and western blotting were performed after 48 h of treatment at 37˚C.

Cell viability. Cell viability was assessed using the Cell Counting Kit-8 (CCK-8; Wuhan Servicebio Technology Co., Ltd.). Briefly, $4x10^3$ cells were plated and treated with high glucose and/or MI-2 as aforementioned for 24 h, followed by incubation with 10% CCK-8 solution for 2 h. Subsequently, the optical density (OD) value was detected using a microplate reader (Nanjing Huadong Electronics Information & Technology Co., Ltd.).

Wound healing assay. The cell migration rate following treatment was assessed using a wound healing assay. Briefly, after treatment, the cells were plated and cultured to achieve 90% confluence. Subsequently, a 10 μl sterile pipette tip was used to create a straight wound across the cell monolayer. After washing, medium containing 1% FBS was added and images of the wound area were captured as baseline (0 h). The cells were then cultured for another 6 h, and images of the wound area were captured again with a light microscope (Motic Industrial Group Co., Ltd.). The width of the wound at 0 and 6 h was measured to calculate the cell migration rate as follows: (Area of wound at 0 h - area of wound at 6 h)/area of wound at 0 h x 100%.

Cell invasion assay. Cell invasion was measured after treatment using a Transwell assay. Briefly, following treatment, the HK-2 cells ($2x10^4$) were resuspended in serum-free medium and were plated in the upper chamber of pre-coated Transwell inserts (0.8 μm, Corning, Inc.). The Transwell inserts were pre-coated with Matrigel matrix (Corning, Inc.) at 37˚C for 1 h. The lower chamber was filled with the standard medium. After 24 h of incubation at 37˚C, the invasive cells were counted after staining with crystal violet solution (Wuhan Servicebio Technology Co., Ltd.) at room temperature for 5 min. Images of the invasive cells were captured with an inverted light microscope (Motic Industrial Group Co., Ltd.).

Immunofluorescence staining. After treatment, the HK-2 cells were washed and fixed in 4% paraformaldehyde solution (Wuhan Servicebio Technology Co., Ltd.) at room temperature for 20 min to preserve cell morphology. The cells were then permeabilized using 0.3% Triton X-100 (Wuhan Servicebio Technology Co., Ltd.) and blocked with bovine serum albumin (Beyotime Institute of Biotechnology) at 37˚C for 1 h. The anti-α-smooth muscle actin (α-SMA) antibody (1:1,000; cat. no. GB111364-50; Wuhan Servicebio Technology Co., Ltd.) was incubated with the cells at 4˚C overnight, and then a Alexa Fluor 488 labeled secondary antibody (1:1,000; cat. no. GB25303; Wuhan Servicebio Technology Co., Ltd.) was incubated with the cells at 37˚C for 30 min, followed by staining with DAPI (Wuhan Servicebio Technology Co., Ltd.) at room temperature for 5 min. An inverted fluorescence microscope (Motic Industrial Group Co., Ltd.) was used to collect images. Relative fluorescence intensity was measured using ImageJ (V1.8.0; National Institutes of Health).

Western blotting. After treatment, the HK-2 cells were washed and the RIPA Kit (Wuhan Servicebio Technology Co., Ltd.) was added to the cells for lysis. Subsequently, the cell lysates were harvested and proteins were isolated after centrifugation at 12,000 x g for 5 min at 4˚C. The protein concentration was quantified using a BCA Kit (Wuhan Servicebio Technology Co., Ltd.). Subsequently, western blotting was performed according to standard procedures, including electrophoresis, electrophoretic transfer, blocking and antibody incubation. Briefly, 20 μg protein was separated by a 4-20% precast gel (Shanghai Willget Biotechnology Co., Ltd.) and transferred to a polyvinylidene difluoride membrane (Merck KGaA). The membrane was blocked with 5% BSA (Wuhan Servicebio Technology Co., Ltd.) at 37˚C for 1 h. Afterwards, the membrane was incubated with primary antibodies overnight at 4˚C and with secondary antibody at 37˚C for 1.5 h. Finally, the signal was detected using an enhanced chemiluminescence kit (Dalian Meilun Biology Technology Co., Ltd.). The antibodies used included: Anti-vimentin (1:50,000; cat. no. 10366-1-AP), anti-inhibitor of κB α (IκBα; 1:10,000; cat. no. 10268-1-AP), anti-phosphorylated (p)-p65 (1:5,000; cat. no. 82335-1-RR) and anti-p65 (1:20,000; cat. no. 80979-1-RR) (all from Wuhan Sanying Biotechnology); anti-E-cadherin (1:2,000; cat. no. AF0131), anti-fibronectin (FN; 1:1,500; cat. no. AF5335) and anti-collagen I (1:2,000; cat. no. AF7001) (all from Affinity Biosciences); and anti-MALT1 (1:1,000; cat. no. GB11790-100), anti-β-actin (1:5,000; cat. no. GB15003-100) and HRP-linked secondary antibodies (1:10,000; cat. no. GB23303) (all from Wuhan

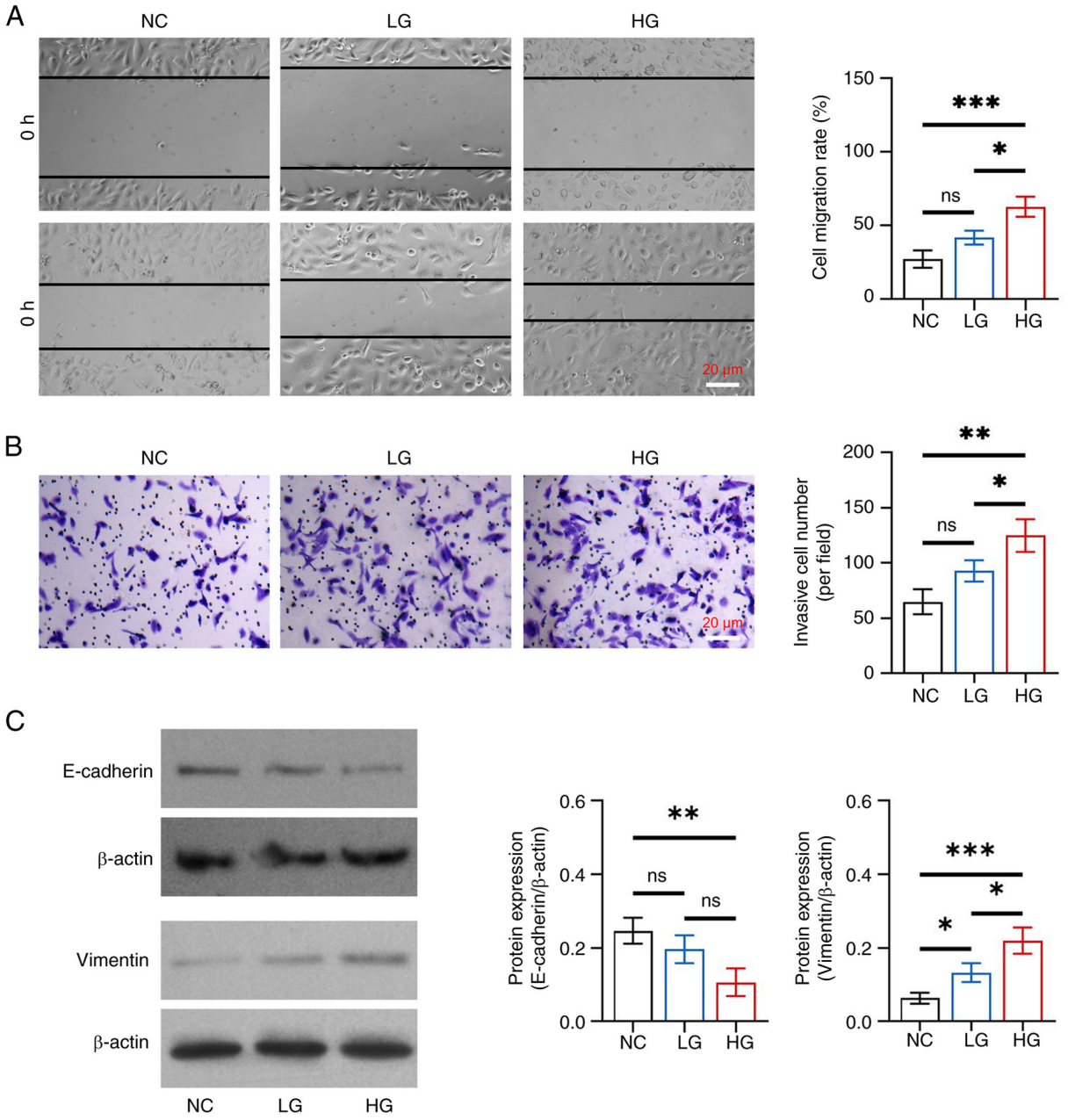

Figure 1. Effect of different concentrations of glucose on epithelial-to-mesenchymal transition in HK-2 cells. (A) Comparison of cell migration rate among the NC, LG and HG groups, between the NC and LG groups, between the NC and HG groups, and between the LG and HG groups. (B) Comparison of invasive cell number among the NC, LG and HG groups, between the NC and LG groups, between the NC and HG groups, and between the LG and HG groups. (C) Comparison of the protein expression levels of E-cadherin among the NC, LG and HG groups, between the NC and LG groups, between the NC and HG groups, and between the LG and HG groups; and comparison of the protein expression levels of vimentin among the NC, LG and HG groups, between the NC and LG groups, between the NC and HG groups, and between the LG and HG groups. *P<0.05, **P<0.01, ***P<0.001; ns, not significant; n=3/group. NC, negative control; LG, low-concentration glucose; HG, high-concentration glucose.

Servicebio Technology Co., Ltd.). The intensity of target bands was assessed using ImageJ software V1.8.0, and the expression levels of the target proteins were normalized to β-actin.

Statistical analysis. Statistical analyses were performed using GraphPad (version 9.0; Dotmatics). The Shapiro-Wilk test of normality was initially performed. Subsequently, group comparisons of normal data were carried out using one-way analysis of variance, followed by Tukey's multiple comparisons test. P<0.05 was considered to indicate a statistically significant difference.

Results

HG facilitates EMT and fibrosis and enhances MALT1 expression in HK-2 cells. In detail, cell migration rate and invasive cell number were increased in the HG group compared with those in the NC and LG groups (all P<0.05), whereas there was no change between the LG and NC groups (both P>0.05) (Fig. 1A and B). Furthermore, E-cadherin protein expression levels were reduced in the HG group compared with those in the NC group (P<0.01), whereas they did not differ between the HG and LG groups, or between the LG and NC groups

(both P>0.05) (Fig. 1C). By contrast, elevated vimentin protein expression was observed in the HG group compared with that in the NC (P<0.001) and LG (P<0.05) groups, as well as in the LG group compared with that in the NC group (P<0.05). These results indicated that glucose promoted EMT with gradient concentration effects in HK-2 cells.

Glucose promoted fibrosis in HK-2 cells in a dose-dependent manner. The relative fluorescence intensity of α-SMA was increased in the HG group compared with that in the NC (P<0.001) and LG (P<0.01) groups, as well as in the LG group compared with in the NC group (P<0.05) (Fig. 2A). In addition, the protein expression levels of FN and collagen I were increased in the HG group compared with those in the NC and LG groups (all P<0.05), but there was no difference in expression between the LG and NC groups (both P>0.05) (Fig. 2B).

Additionally, glucose facilitated MALT1 expression in a dose-dependent manner in HK-2 cells. Specifically, the protein expression levels of MALT1 were increased in the HG group compared with those in the NC (P<0.01) and LG (P<0.05) groups, whereas there was no difference between the LG and NC groups (P>0.05) (Fig. 2C).

MI-2 inhibits cell viability and EMT in HG-treated HK-2 cells. No difference was found in the protein expression levels of MALT1 among the HG, LC-MI-2, MC-MI-2 and HC-MI-2 groups (all P>0.05; Fig. S1), indicating that MI-2 functions by inhibiting MALT1 activity but not its direct expression. However, MI-2 dose-dependently reduced cell viability in HG-treated HK-2 cells, and HC-MI-2 exhibited the best effect. In detail, the OD value was reduced in the HC-MI-2 group compared with that in the HG, LC-MI-2, and MC-MI-2 groups (all P<0.01; Fig. S2). The effect of MI-2 on the inhibition of EMT was dose-dependent in HG-treated HK-2 cells and HC-MI-2 showed the best inhibitory effect. In detail, the cell migration rate and invasive cell number were reduced in the HC-MI-2 group compared with those in the HG and LC-MI-2 groups (all P<0.05), whereas there was no significant difference between the HC-MI-2 group and the MC-MI-2 group (both P>0.05) (Fig. 3A and B). Furthermore, the protein expression levels of E-cadherin were elevated, whereas those of vimentin were reduced in the HC-MI-2 group compared with those in the HG group and the LC-MI-2 group (all P<0.01) (Fig. 3C). Moreover, the protein expression of E-cadherin was elevated in the HC-MI-2 group compared with that in the MC-MI-2 group (P<0.05), but the reduction in vimentin protein expression between the HC-MI-2 and MC-MI-2 groups was not statistically significant (P>0.05).

MI-2 inhibits fibrosis in HG-treated HK-2 cells. MI-2 dose-dependently reduced fibrosis in HG-treated HK-2 cells and HC-MI-2 exhibited the best effect. Specifically, the relative fluorescence intensity of α-SMA was reduced in the HC-MI-2 group compared with that in the HG, LC-MI-2 and MC-MI-2 groups (all P<0.05; Fig. 4A). Furthermore, the protein expression levels of FN were reduced in the HC-MI-2 group compared with those in the HG and LC-MI-2 groups (both P<0.05), but there was no significant difference between the HC-MI-2 group and the MC-MI-2 group (P>0.05) (Fig. 4B). Collagen I protein expression was also decreased in the HC-MI-2 group compared with that in the HG (P<0.001) and LC-MI-2 (P<0.01) groups, but it did not differ statistically between the HC-MI-2 and MC-MI-2 groups (P>0.05).

MI-2 inhibits the NF-κB pathway in HG-treated HK-2 cells. MI-2 inhibited the NF-κB pathway in HG-treated HK-2 cells in a dose-dependent manner and HC-MI-2 had the best inhibitory effect. In particular, IκBα protein expression was increased in the HC-MI-2 group compared with that in the HG (P<0.001), LC-MI-2 (P<0.001) and MC-MI-2 (P<0.05) groups (Fig. 5). By contrast, the protein expression ratio of p-p65/p65 was descended in the HC-MI-2 group compared with that in the HG (P<0.001) and LC-MI-2 (P<0.05) groups; however, no significant difference was found between the HC-MI-2 and MC-MI-2 groups (P>0.05).

Discussion

DN is a burden on healthcare systems that affects ~1/3 of patients with diabetes mellitus (3,17,18). Renal fibrosis, marked by the excessive deposition of extracellular matrix components, destroys kidney structure and causes loss of kidney function, which is closely linked to the development and progression of DN (19). EMT is one of the major pathogeneses of renal fibrosis (20). In the present study, the HK-2 cell line was used, a human renal proximal tubule epithelial cell line, to construct a widely used *in vitro* model of DN (21-25). The results revealed that HG promoted EMT and fibrosis in HK-2 cells, which was similar to the findings of previous studies (22,23). Moreover, previous studies have revealed that HG can induce the protein expression of MALT1, which was similar to the findings of the current study (26,27). In the present study, HG promoted the protein expression levels of MALT1 in HK-2 cells, which indicated that MALT1 may be a promising target and a potential biomarker for DN.

Enhanced cell migration and invasion reflect the development of EMT (28), and the reduction of epithelial surface markers (such as E-cadherin) and the elevation of mesenchymal markers (such as vimentin) are the hallmarks of EMT (29). Furthermore, the excessive deposition of extracellular matrix components, such as α-SMA, FN and collagen I are considered important markers of fibrosis (30). The present study revealed that MI-2 could reverse HG-induced EMT and fibrosis with gradient concentration effects in HK-2 cells. These findings suggested that MI-2 might be an effective therapeutic agent for DN. In the wound healing assay, the choice of time point of cell migration depends on numerous factors. The main factor is the specific requirements of the experiment and cell type. In addition, other factors, such as cell density, scratch width and cell processing methods need to be taken into account. Due to a comprehensive consideration of these factors, the present study set multiple evaluation time points in the preliminary experiments. The time point of 6 h was eventually selected as the evaluation time point to prevent the cells from becoming too dense and affecting the migration evaluation.

The current study suggested that MI-2 did not significantly affect the protein expression of MALT1 in HG-treated HK-2 cells. The cause of this phenomenon may be that MI-2 is an irreversible MALT1 inhibitor, which works by directly combining with MALT1 and inhibiting MALT1 protease activity (15,31-34); thus, MI-2 did not directly affect the protein

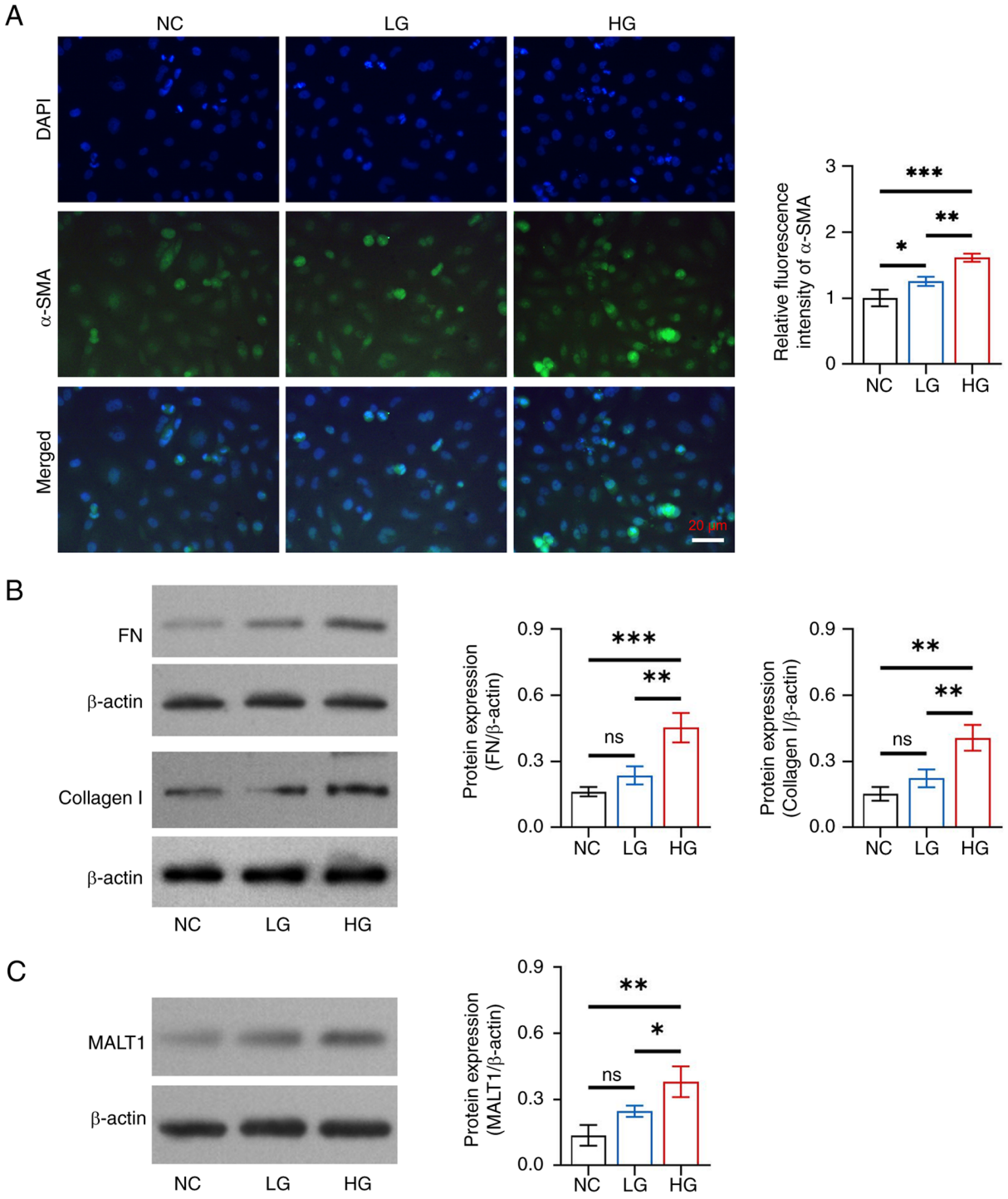

Figure 2. Effects of different concentrations of glucose on fibrosis and MALT1 expression in HK-2 cells. (A) Comparison of the relative fluorescence intensity of α-SMA among the NC, LG and HG groups, between the NC and LG groups, between the NC and HG groups, and between the LG and HG groups. (B) Comparison of the protein expression levels of FN among the NC, LG and HG groups, between the NC and LG groups, between the NC and HG groups, and between the LG and HG groups; and comparison of the protein expression levels of collagen I among the NC, LG and HG groups, between the NC and LG groups, between the NC and HG groups, and between the LG and HG groups. (C) Comparison of the protein expression levels of MALT1 among the NC, LG and HG groups, between the NC and LG groups, between the NC and HG groups, and between the LG and HG groups. *P<0.05, **P<0.01, ***P<0.001; ns, not significant; n=3/group. MALT1, mucosa-associated lymphoid tissue lymphoma translocation protein 1; α-SMA, α-smooth muscle actin; NC, negative control; LG, low-concentration glucose; HG, high-concentration glucose; FN, fibronectin.

expression of MALT1. In addition, due to the fact that MALT1 is the key regulator in activating the NF-κB signaling pathway, the present study further explored whether the NF-κB signaling pathway was inhibited by MI-2 in HG-treated HK-2 cells. The findings revealed that MI-2 increased the protein expression levels of IκBα, while reducing the protein expression ratio of p-p65/p65 in a dose-dependent manner in HG-treated HK-2 cells. Notably, a previous study showed that MALT1 inhibition by MI-2 can suppress the NF-κB signaling pathway in mantle cell lymphoma cells (35). The results of this previous study

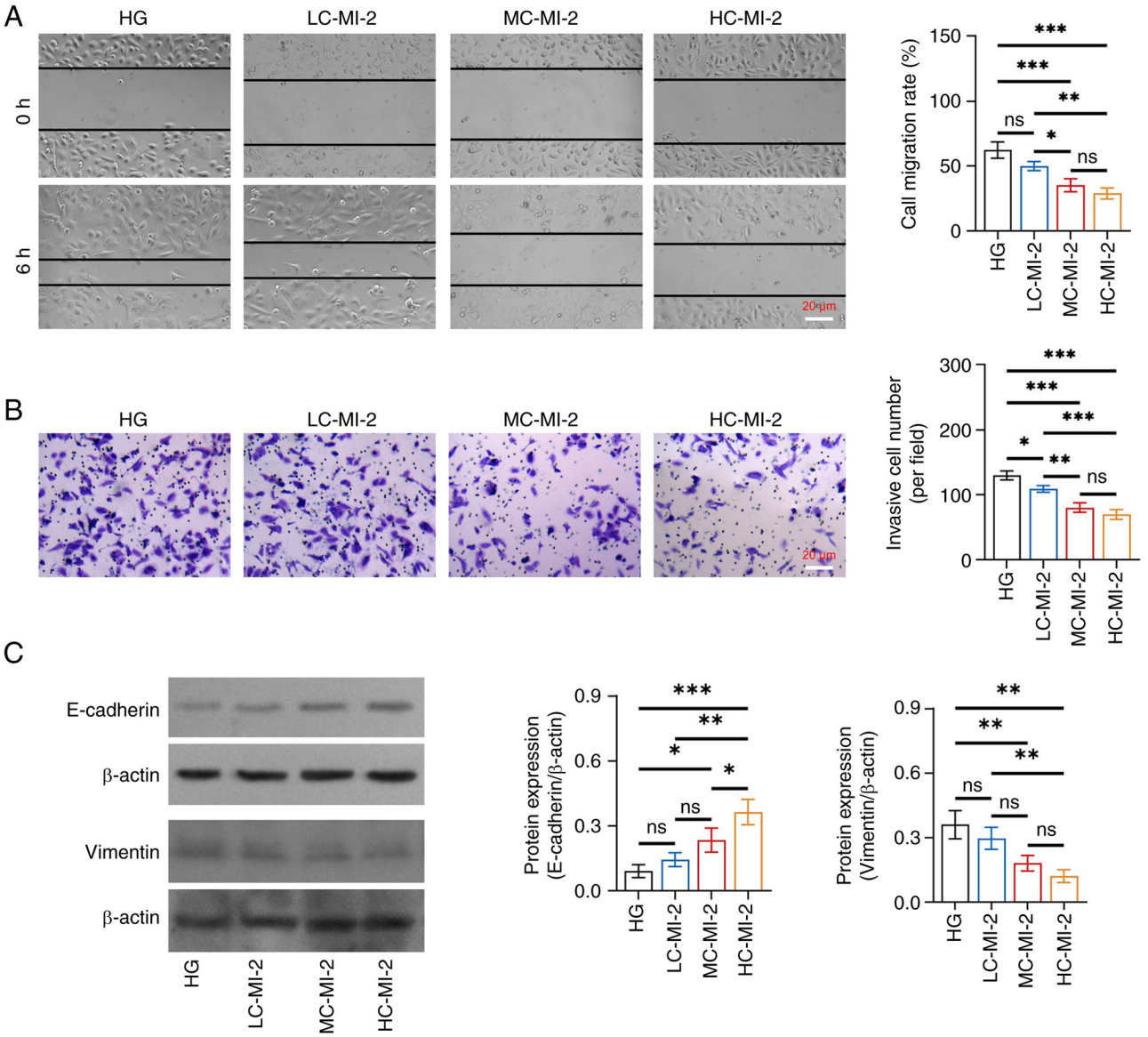

Figure 3. Effect of different concentrations of MI-2 on epithelial-to-mesenchymal transition in HG-treated HK-2 cells. (A) Comparison of cell migration rate among the HG, LC-MI-2, MC-MI-2 and HC-MI-2 groups, between the HG and LC-MI-2 groups, between the HG and MC-MI-2 groups, between the HG and HC-MI-2 groups, between the LC-MI-2 and MC-MI-2 groups, between the LC-MI-2 and HC-MI-2 groups, and between the MC-MI-2 and HC-MI-2 groups. (B) Comparison of invasive cell number among the HG, LC-MI-2, MC-MI-2 and HC-MI-2 groups, between the HG and LC-MI-2 groups, between the HG and MC-MI-2 groups, between the HG and HC-MI-2 groups, between the LC-MI-2 and MC-MI-2 groups, between the LC-MI-2 and HC-MI-2 groups, and between the MC-MI-2 and HC-MI-2 groups. (C) Comparison of the protein expression levels of E-cadherin among the HG, LC-MI-2, MC-MI-2 and HC-MI-2 groups, between the HG and LC-MI-2 groups, between the HG and MC-MI-2 groups, between the HG and HC-MI-2 groups, between the LC-MI-2 and MC-MI-2 groups, between the LC-MI-2 and HC-MI-2 groups, and between the MC-MI-2 and HC-MI-2 groups; and comparison of the protein expression levels of vimentin among the HG, LC-MI-2, MC-MI-2 and HC-MI-2 groups, between the HG and LC-MI-2 groups, between the HG and MC-MI-2 groups, between the HG and HC-MI-2 groups, between the LC-MI-2 and MC-MI-2 groups, between the LC-MI-2 and HC-MI-2 groups, and between the MC-MI-2 and HC-MI-2 groups. HK-2 cells in the LC-MI-2, MC-MI-2 and HC-MI-2 groups were treated with HG. *P<0.05, **P<0.01, ***P<0.001; ns, not significant; n=3/group. HG, high-concentration glucose; LC-MI-2, low concentration MI-2; MC-MI-2, medium concentration MI-2; HC-MI-2; high concentration MI-2.

were similar to the present results (35), indicating that MALT1 inhibition by MI-2 may decrease cell viability and migration via the NF-κB signaling pathway. However, there were some differences between the previous study and the current study: i) The previous study focused on mantle cell lymphoma cells, whereas the present study focused on HK-2 cells (which were used for *in vitro* studies of DN) (35). ii) The previous study highlighted the impact of MI-2 inhibiting the NF-κB signaling pathway on tumor resistance, while the present study focused on its impact on EMT and fibrosis (35). iii) The previous study did not construct MI-2 concentration gradient models; however, the present study constructed these models, which further indicated that the inhibitory effect of MI-2 on the NF-κB pathway was dose-dependent (35). The possible mechanisms underlying the inhibitory effects of MI-2 on the NF-κB signaling pathway may be as follows: MI-2 could directly bind to MALT1 and suppress its protease function, thus disrupting the assembly of the CARMA1/BCL10/MALT1 (CBM) complex, further inactivating the IκB kinase complex, inhibiting the phosphorylation of IκB and reducing NF-κB activation (36,37). However, the current study did not explore specific molecular interactions or downstream effects, which

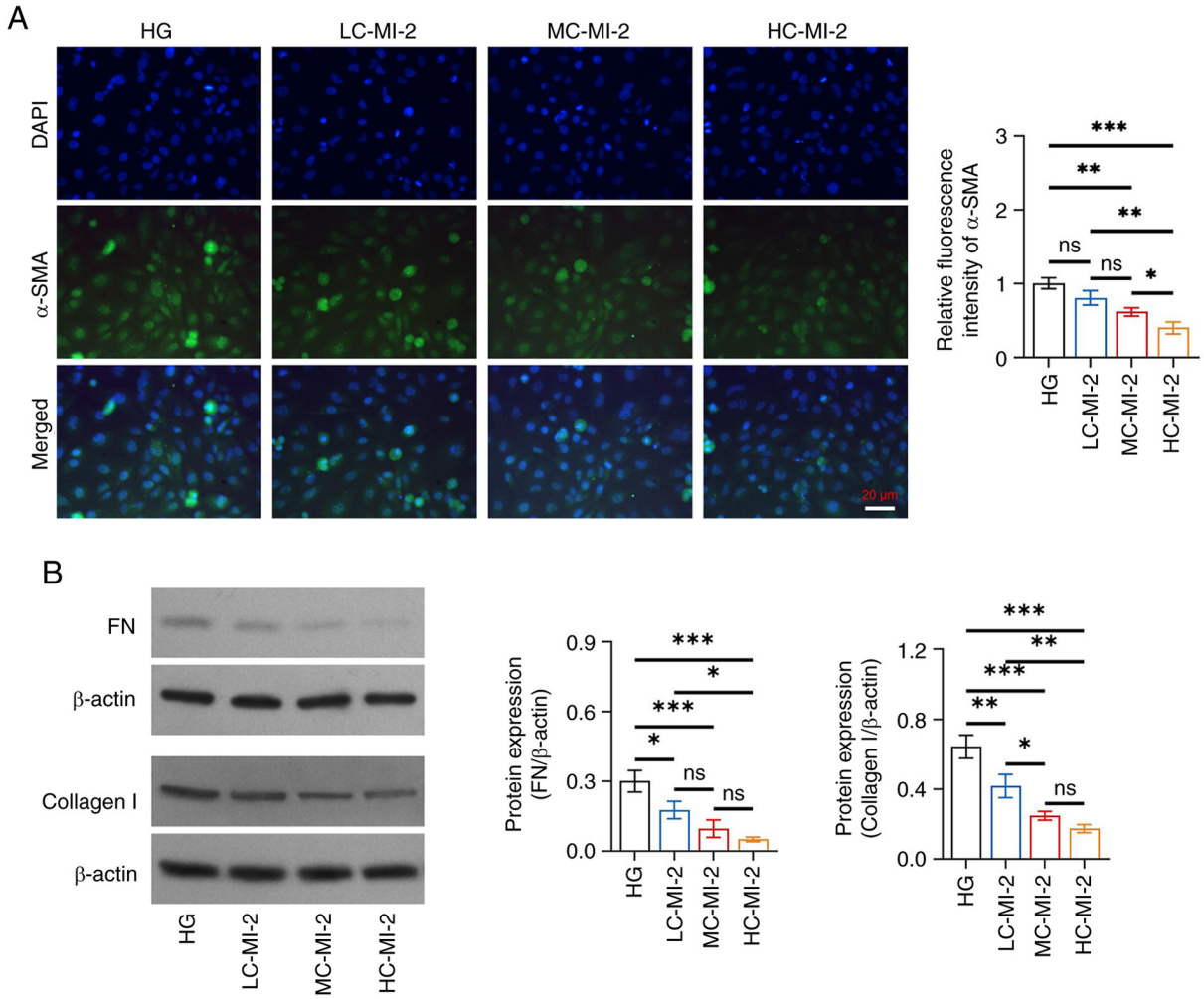

Figure 4. Effect of different concentrations of MI-2 on fibrosis in HG-treated HK-2 cells. (A) Comparison of the relative fluorescence intensity of α-SMA among the HG, LC-MI-2, MC-MI-2 and HC-MI-2 groups between the HG and LC-MI-2 groups, between the HG and MC-MI-2 groups, between the HG and HC-MI-2 groups, between the LC-MI-2 and MC-MI-2 groups, between the LC-MI-2 and HC-MI-2 groups, and between the MC-MI-2 and HC-MI-2 groups. (B) Comparison of the protein expression levels of FN among the HG, LC-MI-2, MC-MI-2 and HC-MI-2 groups, between the HG and LC-MI-2 groups, between the HG and MC-MI-2 groups, between the HG and HC-MI-2 groups, between the LC-MI-2 and MC-MI-2 groups, between the LC-MI-2 and HC-MI-2 groups, and between the MC-MI-2 and HC-MI-2 groups; and comparison of the protein expression levels of collagen I among the HG, LC-MI-2, MC-MI-2 and HC-MI-2 groups, between the HG and LC-MI-2 groups, between the HG and MC-MI-2 groups, between the HG and HC-MI-2 groups, between the LC-MI-2 and MC-MI-2 groups, between the LC-MI-2 and HC-MI-2 groups, and between the MC-MI-2 and HC-MI-2 groups. HK-2 cells in the LC-MI-2, MC-MI-2 and HC-MI-2 groups were treated with HG. *P<0.05, **P<0.01, ***P<0.001; ns, not significant; n=3/group. HG, high-concentration glucose; α-SMA, α-smooth muscle actin; LC-MI-2, low concentration MI-2; MC-MI-2, medium concentration MI-2; HC-MI-2; high concentration MI-2; FN, fibronectin.

require verification in future studies. Overall, the results indicated that MI-2 inhibited MALT1, further blocking the NF-κB signaling pathway to suppress HG-induced EMT and fibrosis. Notably, some other signaling pathways, such as transforming growth factor-β/SMAD, Wnt/β-catenin and phosphatidylinositol 3-kinase/protein kinase B/mammalian target of the rapamycin, are also involved in EMT and fibrosis (38-40). These signaling pathways could be explored in future studies.

Overall, the aforementioned findings highlighted that MI-2 might be a promising agent, which could meet the current clinical needs for the management of DN. However, the CCK-8 cell viability assay showed that MI-2 dose-dependently reduced the viability of HG-treated HK-2 cells. This result indicated that although MI-2 showed a favorable effect on the treatment of DN, its clinical application may be limited by toxicity. Thus, strict dose optimization is required to avoid exacerbating toxicity in clinical practice. Moreover, more clinical studies are required to further validate the clinical application of MI-2, including the efficacy and safety assessment of MI-2 in patients with DN.

The current study has the following limitations: i) The mechanism by which HG promoted the protein expression of MALT1 in HK-2 cells remains unknown. Future studies should explore the signaling pathways or transcription factors involved in MALT1 upregulation under HG conditions, which may provide deeper insights into the pathogenesis of DN and potential therapeutic targets. ii) The study only focused on HK-2 cells. The findings may not be generalizable to other types of kidney cells, such as podocytes and mesangial cells, which also serve crucial roles in DN. Thus, future studies should investigate whether MI-2 has similar effects on these kidney cells. iii) Due to the lack of experimental conditions, the current study was entirely based on *in vitro* experiments. The results might not fully reflect the complex interactions

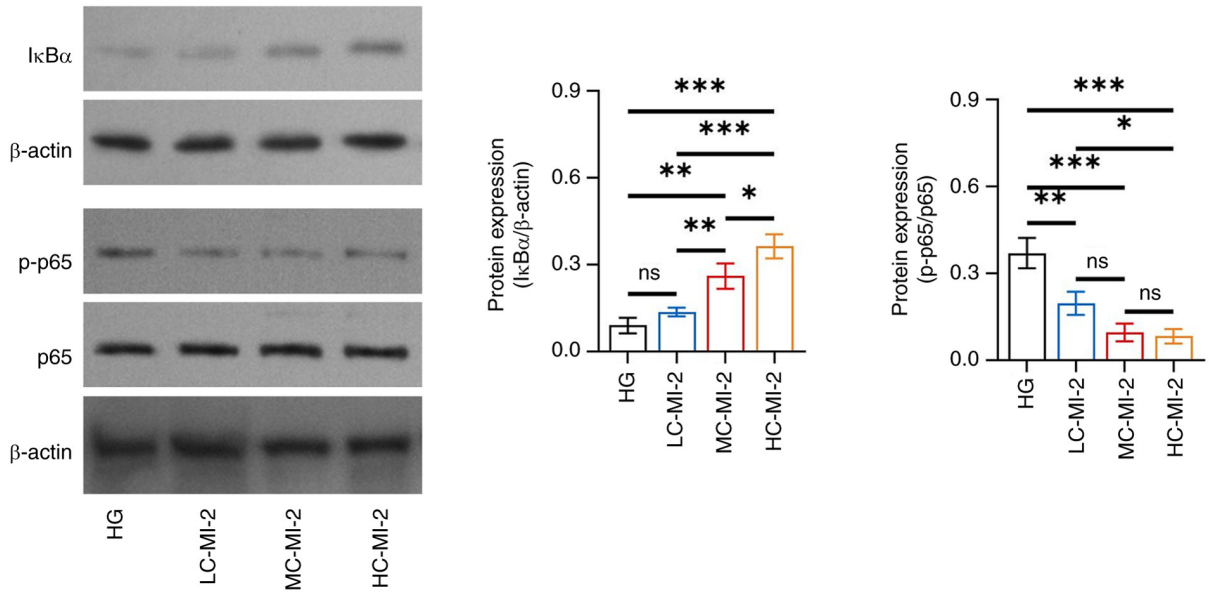

Figure 5. Effect of different concentrations of MI-2 on the NF-κB pathway in HG-treated HK-2 cells. Comparison of the protein expression levels of IκBα among the HG, LC-MI-2, MC-MI-2 and HC-MI-2 groups, between the HG and LC-MI-2 groups, between the HG and MC-MI-2 groups, between the HG and HC-MI-2 groups, between the LC-MI-2 and MC-MI-2 groups, between the LC-MI-2 and HC-MI-2 groups, and between the MC-MI-2 and HC-MI-2 groups; and comparison of p-p65/p65 among the HG, LC-MI-2, MC-MI-2 and HC-MI-2 groups, between the HG and LC-MI-2 groups, between the HG and MC-MI-2 groups, between the HG and HC-MI-2 groups, between the LC-MI-2 and MC-MI-2 groups, between the LC-MI-2 and HC-MI-2 groups, and between the MC-MI-2 and HC-MI-2 groups. HK-2 cells in the LC-MI-2, MC-MI-2 and HC-MI-2 groups were treated with HG. *P<0.05, **P<0.01, ***P<0.001; ns, not significant; n=3/group. HG, high-concentration glucose; IκBα, inhibitor of κB α; LC-MI-2, low concentration MI-2; MC-MI-2, medium concentration MI-2; HC-MI-2; high concentration MI-2; p, phosphorylated.

and responses in a living organism. Future studies should conduct *in vivo* studies using animal models of DN to validate the findings and assess the therapeutic potential of MI-2 in a more physiologically relevant context. iv) The current study evaluated the effects of MI-2 treatment after 48 h, and the short duration might not capture the full spectrum of cellular responses or long-term effects. Future studies should extend the treatment and observation periods to evaluate the sustained effects and potential side effects of MI-2. v) The current study lacked detailed mechanistic studies to elucidate the specific interactions and downstream effects of MALT1 inhibition by MI-2 on the NF-κB pathway. On one hand, MALT1 acts as a scaffolding protein, which mediates the formation of the CBM complex to drive activation of the NF-κB pathway (41). Thus, immunoprecipitation is required to evaluate the effect of MALT1 on the CBM complex, and western blot analysis should be performed to assess the effect of MI-2 on downstream proteins of the CBM complex (such as TRAF6 and TAK1). On the other hand, MALT1 acts as a protease, which cleaves several proteins directly connected to the NF-κB pathway, such as CYLD, A20 and RelB (41). Thus, western blotting is required to assess the effect of MI-2 on these related proteins. However, considering technical and financial limitations, the detailed molecular studies were not conducted. vi) Due to financial limitations, the current study prioritized and only focused on the NF-κB pathway. Future studies may consider investigating other relevant signaling pathways to provide a more comprehensive understanding of the molecular mechanisms. vii) The current study only used western blotting to measure proteins, whereas dual measurements of proteins using enzyme-linked immunosorbent assay and western blotting assay may enhance the quality of results.

In conclusion, the present study revealed that MALT1 inhibition by MI-2 may attenuate HG-induced EMT and fibrosis in HK-2 cells, and this attenuation may be attributed to inhibition of the NF-κB signaling pathway.

Acknowledgements

Not applicable.

Funding

This study was supported by the Postdoctoral Foundation of Heilongjiang Province (grant no. LBH-Z23284), Heilongjiang University of Chinese Medicine Young Researchers Scientific and Technological Innovation Capacity Cultivation Project (grant nos. 2024XJJ-QNCX023 and 2024-KYYWF-1392), Heilongjiang University of Traditional Chinese Medicine 'Double First Class' Discipline Development Assistance Fund (grant no. GJJGSPZDXK31003) and the NSFC Cultivation Support Program, First Affiliated Hospital, Heilongjiang University of Chinese Medicine (grant no. PYQN202501008).

Availability of data and materials

The data generated in the present study may be requested from the corresponding author.

Authors' contributions

NZ contributed to the conception and the design of the study. YL and JM were responsible for the acquisition and analysis of the data. HC and CL contributed to data interpretation. All

authors contributed to manuscript drafting or critical revisions of the intellectual content. NZ and YL confirm the authenticity of all the raw data. All authors read and approved the final version of the manuscript.

Ethics approval and consent to participate

Not applicable.

Patient consent for publication

Not applicable.

Competing interests

The authors declare that they have no competing interests.

References

1. Caramori ML and Rossing P: Diabetic Kidney Disease. In: Endotext. Feingold KR, Anawalt B, Blackman MR, Boyce A, Chrousos G, Corpas E, de Herder WW, Dhatariya K, Dungan K, Hofland J, Kalra S, Kaltsas G, Kapoor N, Koch C, Kopp P, Korbonits M, Kovacs CS, Kuohung W, Laferrere B, Levy M, McGee EA, McLachlan R, New M, Purnell J, Sahay R, Shah AS, Singer F, Sperling MA, Stratakis CA, Trence DL and Wilson DP (eds). South Dartmouth (MA), 2000.
2. Dwivedi S and Sikarwar MS: Diabetic nephropathy: Pathogenesis, mechanisms, and therapeutic strategies. Horm Metab Res 57: 7-17, 2025.
3. Hu Q, Chen Y, Deng X, Li Y, Ma X, Zeng J and Zhao Y: Diabetic nephropathy: Focusing on pathological signals, clinical treatment, and dietary regulation. Biomed Pharmacother 159: 114252, 2023.
4. Zac-Varghese S, Mark P, Bain S, Banerjee D, Chowdhury TA, Dasgupta I, De P, Fogarty D, Frankel A, Goldet G, *et al*: Clinical practice guideline for the management of lipids in adults with diabetic kidney disease: Abbreviated summary of the Joint Association of British Clinical Diabetologists and UK Kidney Association (ABCD-UKKA) Guideline 2024. BMC Nephrol 25: 216, 2024.
5. Zeng LF, Xiao Y and Sun L: A glimpse of the mechanisms related to renal fibrosis in diabetic nephropathy. Adv Exp Med Biol 1165: 49-79, 2019.
6. Watanabe K, Sato E, Mishima E, Miyazaki M and Tanaka T: What's new in the molecular mechanisms of diabetic kidney disease: Recent advances. Int J Mol Sci 24: 570, 2022.
7. Jonckheere S, Adams J, De Groote D, Campbell K, Berx G and Goossens S: Epithelial-mesenchymal transition (EMT) as a therapeutic target. Cells Tissues Organs 211: 157-182, 2022.
8. Chen Y, Zou H, Lu H, Xiang H and Chen S: Research progress of endothelial-mesenchymal transition in diabetic kidney disease. J Cell Mol Med 26: 3313-3322, 2022.
9. Balakumar P, Sambathkumar R, Mahadevan N, Muhsinah AB, Alsayari A, Venkateswaramurthy N and Jagadeesh G: A potential role of the renin-angiotensin-aldosterone system in epithelial-to-mesenchymal transition-induced renal abnormalities: Mechanisms and therapeutic implications. Pharmacol Res 146: 104314, 2019.
10. Hadpech S and Thongboonkerd V: Epithelial-mesenchymal plasticity in kidney fibrosis. Genesis 62: e23529, 2024.
11. Zhang YY, Peng J and Luo XJ: Post-translational modification of MALT1 and its role in B cell- and T cell-related diseases. Biochem Pharmacol 198: 114977, 2022.
12. Afonina IS, Elton L, Carpentier I and Beyaert R: MALT1-a universal soldier: Multiple strategies to ensure NF-κB activation and target gene expression. FEBS J 282: 3286-3297, 2015.
13. Hachmann J and Salvesen GS: The Paracaspase MALT1. Biochimie 122: 324-338, 2016.
14. Lee JL, Ekambaram P, Carleton NM, Hu D, Klei LR, Cai Z, Myers MI, Hubel NE, Covic L, Agnihotri S, *et al*: MALT1 is a targetable driver of epithelial-to-mesenchymal transition in claudin-low, triple-negative breast cancer. Mol Cancer Res 20: 373-386, 2022.
15. Fusco R, Siracusa R, D'Amico R, Cordaro M, Genovese T, Gugliandolo E, Peritore AF, Crupi R, Di Paola R, Cuzzocrea S and Impellizzeri D: Mucosa-associated lymphoid tissue lymphoma translocation 1 inhibitor as a novel therapeutic tool for lung injury. Int J Mol Sci 21: 7761, 2020.
16. Fontan L, Yang C, Kabaleeswaran V, Volpon L, Osborne MJ, Beltran E, Garcia M, Cerchietti L, Shaknovich R, Yang SN, *et al*: MALT1 small molecule inhibitors specifically suppress ABC-DLBCL in vitro and in vivo. Cancer Cell 22: 812-824, 2012.
17. Elendu C, John Okah M, Fiemotongha KDJ, Adeyemo BI, Bassey BN, Omeludike EK and Obidigbo B: Comprehensive advancements in the prevention and treatment of diabetic nephropathy: A narrative review. Medicine (Baltimore) 102: e35397, 2023.
18. Samsu N: Diabetic nephropathy: Challenges in pathogenesis, diagnosis, and treatment. Biomed Res Int 2021: 1497449, 2021.
19. Huang R, Fu P and Ma L: Kidney fibrosis: From mechanisms to therapeutic medicines. Signal Transduct Target Ther 8: 129, 2023.
20. Cao Y, Lin JH, Hammes HP and Zhang C: Cellular phenotypic transitions in diabetic nephropathy: An update. Front Pharmacol 13: 1038073, 2022.
21. Huang J, Chen G, Wang J, Liu S and Su J: Platycodin D regulates high glucose-induced ferroptosis of HK-2 cells through glutathione peroxidase 4 (GPX4). Bioengineered 13: 6627-6637, 2022.
22. Li J, Shu L, Jiang Q, Feng B, Bi Z, Zhu G, Zhang Y, Li X and Wu J: Oridonin ameliorates renal fibrosis in diabetic nephropathy by inhibiting the Wnt/β-catenin signaling pathway. Ren Fail 46: 2347462, 2024.
23. Zeng J and Bao X: Tanshinone IIA attenuates high glucose-induced epithelial-to-mesenchymal transition in HK-2 cells through VDR/Wnt/β-catenin signaling pathway. Folia Histochem Cytobiol 59: 259-270, 2021.
24. Sun Y, Qu H, Song Q, Shen Y, Wang L and Niu X: High-glucose induced toxicity in HK-2 cells can be alleviated by inhibition of miRNA-320c. Ren Fail 44: 1388-1398, 2022.
25. Deng J, Zheng C, Hua Z, Ci H, Wang G and Chen L: Diosmin mitigates high glucose-induced endoplasmic reticulum stress through PI3K/AKT pathway in HK-2 cells. BMC Complement Med Ther 22: 116, 2022.
26. Chen ST, Chang KS, Lin YH, Hou CP, Lin WY, Hsu SY, Sung HC, Feng TH, Tsui KH and Juang HH: Glucose upregulates ChREBP via phosphorylation of AKT and AMPK to modulate MALT1 and WISP1 expression. J Cell Physiol 240: e31478, 2025.
27. Wang X, Gao Y, Sun H, *et al*: Mechanism of Tangluoning for alleviating high glucose-induced inflammatory reaction of Schwann cells by regulating lncRNA MALAT1. Beijing Journal of Traditional Chinese Medicine 41: 236-239, 2022 (In Chinese).
28. Yang J, Antin P, Berx G, Blanpain C, Brabletz T, Bronner M, Campbell K, Cano A, Casanova J, Christofori G, *et al*: Guidelines and definitions for research on epithelial-mesenchymal transition. Nat Rev Mol Cell Biol 21: 341-352, 2020.
29. Serrano-Gomez SJ, Maziveyi M and Alahari SK: Regulation of epithelial-mesenchymal transition through epigenetic and post-translational modifications. Mol Cancer 15: 18, 2016.
30. Meran S and Steadman R: Fibroblasts and myofibroblasts in renal fibrosis. Int J Exp Pathol 92: 158-167, 2011.
31. Zhang H, Sun G, Li X, Fu Z, Guo C, Cao G, Wang B, Wang Q, Yang S, Li D, *et al*: Inhibition of MALT1 paracaspase activity improves lesion recovery following spinal cord injury. Sci Bull (Beijing) 64: 1179-1194, 2019.
32. Yan B, Belke D, Gui Y, Chen YX, Jiang ZS and Zheng XL: Pharmacological inhibition of MALT1 (mucosa-associated lymphoid tissue lymphoma translocation protein 1) induces ferroptosis in vascular smooth muscle cells. Cell Death Discov 9: 456, 2023.
33. Gu H, Qiu H, Yang H, Deng Z, Zhang S, Du L and He F: PRRSV utilizes MALT1-regulated autophagy flux to switch virus spread and reserve. Autophagy 20: 2697-2718, 2024.
34. Li Y, Huang X, Huang S, He H, Lei T, Saaoud F, Yu XQ, Melnick A, Kumar A, Papasian CJ, *et al*: Central role of myeloid MCPIP1 in protecting against LPS-induced inflammation and lung injury. Signal Transduct Target Ther 2: 17066, 2017.
35. Jiang VC, Liu Y, Lian J, Huang S, Jordan A, Cai Q, Lin R, Yan F, McIntosh J, Li Y, *et al*: Cotargeting of BTK and MALT1 overcomes resistance to BTK inhibitors in mantle cell lymphoma. J Clin Invest 133: e165694, 2023.

36. Qian R, Niu X, Wang Y, Guo Z, Deng X, Ding Z, Zhou M and Deng H: Targeting MALT1 suppresses the malignant progression of colorectal cancer via miR-375/miR-365a-3p/NF-κB axis. Front Cell Dev Biol 10: 845048, 2022.
37. Yao Y, Yuan M, Shi M, Li W, Sha Y, Zhang Y, Yuan C, Luo J, Li Z, Liao C, *et al*: Halting multiple myeloma with MALT1 inhibition: suppressing BCMA-induced NF-κB and inducing immunogenic cell death. Blood Adv 8: 4003-4016, 2024.
38. Lee JH and Massague J: TGF-β in developmental and fibrogenic EMTs. Semin Cancer Biol 86: 136-145, 2022.
39. Hu L, Ding M and He W: Emerging therapeutic strategies for attenuating tubular EMT and kidney fibrosis by targeting Wnt/β-catenin signaling. Front Pharmacol 12: 830340, 2022.
40. Lu Q, Wang WW, Zhang MZ, Ma ZX, Qiu XR, Shen M and Yin XX: ROS induces epithelial-mesenchymal transition via the TGF-β1/PI3K/Akt/mTOR pathway in diabetic nephropathy. Exp Ther Med 17: 835-846, 2019.
41. Moud BN, Ober F, O'Neill TJ and Krappmann D: MALT1 substrate cleavage: What is it good for? Front Immunol 15: 1412347, 2024.